ELASTIC-PLASTIC FINITE ELEMENT SIMULATION OF CRACK TIP DEFORMATION IN FATIGUE

M.M.I. HAMMOUDA
Mech. Eng. Dept., Al Azhar University, Cairo, Egypt
H.E.M. SALLAM
Eng. Mat. Dept., Zagazig University, Zagazig, Egypt

ABSTRACT

An elastic-plastic finite element model was developed to simulate the deformation behaviour at the tip and of the surface of a long crack in fatigue. Both stationary and propagating fatigue crack were analysed and compared in terms of plastically deformed zones and crack surface deformation. The model accommodates crack tip opening displacement and both crack tip and crack edge closure. Crack tip deformation was utilized to correlate FCG rates of geometrically different specimens made of three materials tested at different stress ranges and R-ratios.

KEYWORDS

Finite element analysis, crack tip plastic deformation, stationary fatigue crack, crack closure, fatigue crack growth.

INTRODUCTION

The closure factor U, = $(\sigma_{max} - \sigma_{op})/(\sigma_{max} - \sigma_{min})$, has been used to compensate for the crack tip closure in the correlation of fatigue crack growth rates. The problem with this complicating factor is the need of its calibration for each case under consideration. It depends on the nature of the applied stress cycles, the properties of the material and the geometry of both the specimen and the crack surface (**Suzuki et al., 1991**). A lack of definition is obvious when partial closure takes place.

Problems associated with accurate experimental measurements relevant to closure were demonstrated (**Bowman et al., 1988**). Numerically, the finite element method (FEM) was invoked to study plasticity induced crack tip closure (**McClung, 1991**). The main aim of such works were to search for U and its effects on some parameters in relation to the behaviour of a fatigue crack.

Fatigue crack growth (FCG) is controlled by cyclic crack tip deformation (CTD) (**Tanaka et al., 1984**). Thus, knowing this CTD during a load cycle is useful in resolving the problem of

correlating FCG rates. In this respect, the FEM is a powerful tool having the advantage of closely approaching the crack tip (**Nakamura et al., 1989**). In the present work, the deformation behaviour at the tip and of the surface of stationary and propagating fatigue cracks is analysed.

FINITE ELEMENT SIMULATION

FCG at different stress ratios was simulated by a two-dimensional elastic-plastic finite element model. Elastic properties typical of steels and a yield stress, σ_y, of 350 MPa were used. In the plastic regime the stress-plastic strain, σ-ε_p, behaviour of the material was assumed to obey a simple power law with a strain hardening exponent of 0.2. The commonly used Von-Mises yield criterion and the Prandtle-Reuss flow rule were adopted. The Bauschinger effect was considered through the kinematic hardening model modified by **Ziegler (1959)**.

The analysis was performed for an axially loaded plate with the dimensions of 300mm x 50mm having a single edge crack with a length to width ratio = 0.5. A mesh of constant stress triangular elements was adopted with 756 degrees of freedom. A number of 400 elements of size to crack length ratio of 0.0025 were constructed around the crack tip. The plane stress state was assumed.

The response of such a plate was analysed for loading cycles with the following sequence. The first half cycle represented a monotonic loading of a stationary crack. Two stress cycles were further applied on that crack. The sequence of incremental cracking-unloading-reloading was invoked for the next cycles. The crack was allowed to extend at the point of maximum load by an incremental release of the existing crack tip reaction force. Cracking increment to width ratio was 0.00125.

Deformation around the crack tip was incrementally traced. The model accommodated the closure phenomenon at both the edge and the tip of the crack. Generally, the load increment was adjusted to have either one further plastically deformed element or a change in the crack surface contact whichever took the lead.

RESULTS AND DISCUSSION

Behaviour of a Stationary Crack. The change in crack surface profile due to the application of the first half monotonic load cycle is shown in Fig. 1. The opening of the crack at the node just behind the crack tip was employed for the calculation of the crack tip opening displacement (CTOD), δ, as given in Fig. 2. The monotonic development of the crack tip plastic zone was traced.. Its size, Δ_m, was considered as the diameter of a circle of the same area. The extent of Δ_m could be expressed in terms of stress level. The extents of both δ and Δ_m are related by

$$\delta / a Y^2 = 1.336\, \varepsilon_y (\Delta_m / a Y^2)^{0.852} \qquad (1)$$

where ε_y is the yield strain of the material. The normalization utilized in the above equation is of interest. The geometry of both the crack tip and the component as well as the type of loading are reflected by the geometrical factor Y commonly used in the mathematical definition of the stress intensity factor.

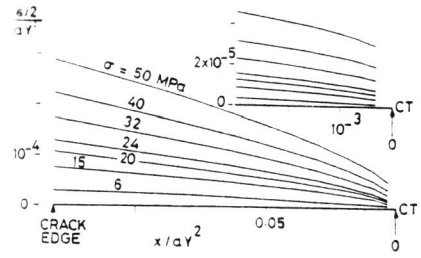

Fig. 1. Profile of a stationary crack due to the application of the first of half cycle

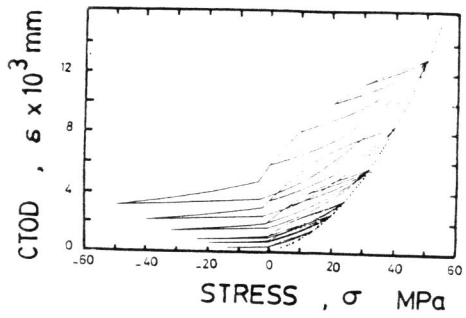

Fig. 2. CTOD of a stationary fatigue crack due to different loading-unloading and reloading cycles

Fig. 2 depicts the extent of δ in the course of different schemes for the first unloading-reloading cycle. The sudden changes in the compliance was due to the occurrence of crack edge closure and its following reopening. This is illustrated by the variation in the crack surface profile typified in Fig. 3. The crack closes continuously from its edge to near the tip as found by **Ohji et al (1975)**. A relatively high compressive load dependent on the maximum extent of δ, δ_s, is necessary for complete closure.

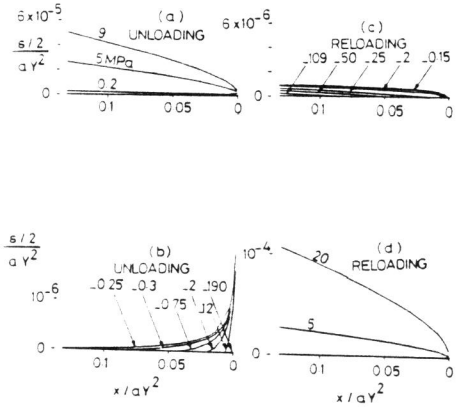

Fig. 3. Profile of stationary fatigue crack due to the first unloading-reloading cycle

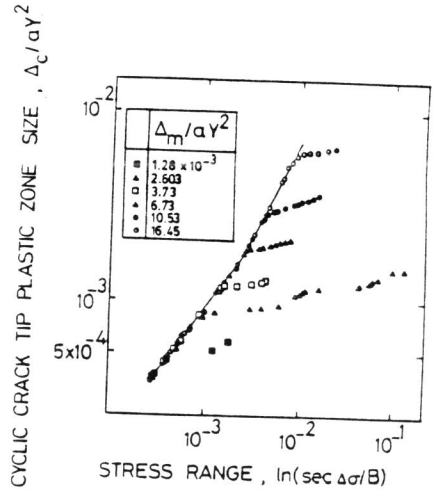

Fig. 4. Extent of the reversed plastic zone formed at the tip of a stationary fatigue crack

The reversed plastic zones were traced and its corresponding size, Δ_c, is related in Fig. 4 to the stress range, $\Delta\sigma$. The solid line shown on that figure represents fully opened crack. The deviation from that line indicates the development of crack edge closure. It is obvious that there is a critical value for Δ_c dependent on Δ_m and crack length beyond which crack edge closure is developed as indicated by the upper line of Fig. 5.

Tomkins model (**Tomkins, 1991**) suggests the presentation of the cyclic CTOD, $\Delta\delta$, in the nondimensional form shown in Fig. 6. Here, T is the cyclic ultimate stress ($\approx 2\sigma_y$). The data on

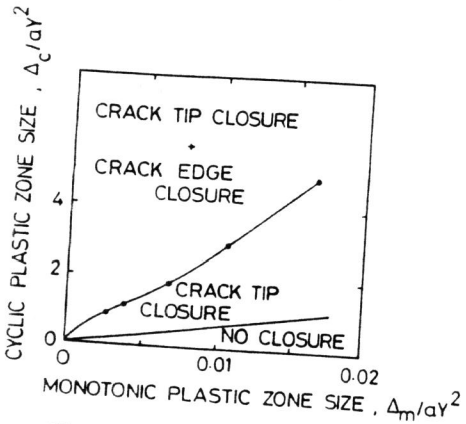

Fig. 5. Possible regimes of crack surface closure in fatigue

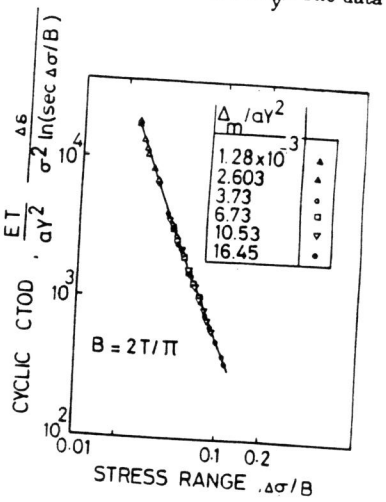

Fig. 6. A nondimensional presentation of cyclic CTOD of a stationary fatigue crack

that figure represent the fully opened stationary crack for which $\Delta\delta$ and Δ_c could be correlated as presented by the solid line in Fig. 7. The data presented in that figure indicate that such a correlation could be invoked for partially opened crack. Obviously, the limitation here corresponds to $\Delta\delta = \delta_s$ representing the case of a fully closed crack. Fig. 2 shows clearly that the ratio $\Delta\delta/\delta s$ decreases as δs increases. This ratio approached unity at very low values of δ_s.

The response in terms of $\Delta\delta$ and Δ_c due to the application of the second stress cycle closely doubled back that of the first cycle indicating a case of quick stabilization.

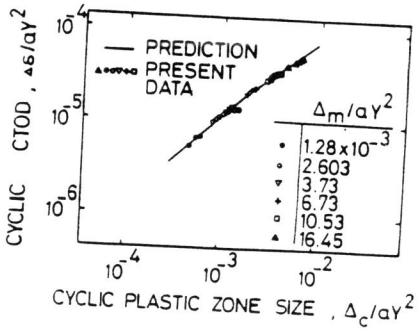

Fig. 7. Correlation of cyclic CTOD and cyclic crack tip plastic zone for a stationary fatigue crack

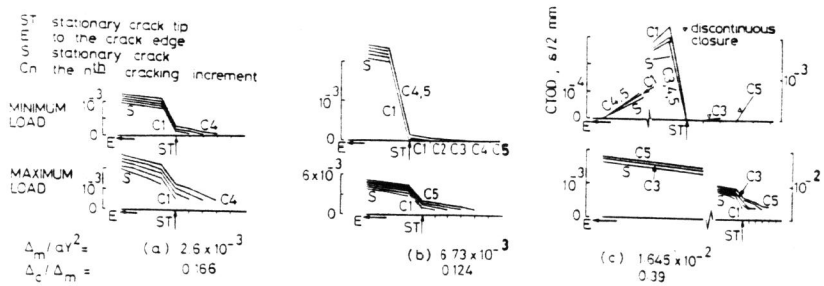

Fig. 8. Examples of surface profiles of a propagating fatigue crack at both minimum and maximum loads corresponding to three different cycles.

Simulation of a Propagating Fatigue Crack. The deformation of the surface and around the tip of the crack was traced in the course of each series of cracking, unloading and reloading phases. Three different plastic zones could be distinguished at the termination of the above three phases, i.e. cracking plastic zone (CPZ), unloading plastic zone (UPZ) and reloading plastic zone (LPZ). Due to cracking and unloading, the extent of the LPZ and UPZ were less than the monotonic and the cyclic plastic zones of a stationary crack of the same depth. The least extent amongst the three zones corresponded to the unloading phase. The LPZ was of a size less than that of the CPZ. This is due to the elastic cyclic response during unloading and reloading of the material located near the elastic-plastic boundary of the CPZ.

Corresponding crack surface profiles are demonstrated in Fig. 8 for three of the analysed load cases after the execution of their sequent unloading and reloading phases. Both crack tip and crack edge closure were possible. In this case, crack tip closure took the lead starting just behind the tip to shut a number of nodes on the cracked area depending on the minimum stress. Similar results are reported in the literature (**Ohji et al., 1975**). The phenomenon of crack edge closure accorded with that of a stationary crack of the same length, see Fig. 5. In this case, Δ_m and Δc correspond to those of that stationary crack. For a given maximum load the stabilized minimum CTOD decreased with a corresponding decrease in the R-ratio. These data were best fitted to conclude the critical condition delineated in Fig. 9 to develop crack tip closure in the present specimen. In that figure, Δa is used to normalize Δ_m for the cracking increment is known to have an effect on closure results (**Newman, 1976**). The implication here is that crack tip closure can be accommodated at a lower value of Δ_c/Δ_m for a larger extent of Δ_m. However, in actual fatigue loading $\Delta_m/\Delta a$ is very large and according to Fig. 9 the critical value of Δ_c/Δ_m is about 0.0625. This condition is indicated by the lower line in Fig. 5 which illustrates three possible regimes relevant to crack surface closure.

The cyclic CTOD, $\Delta\delta$, after cracking is plotted in Fig. 10 against the additional cracked length, $\Delta\ell$. In that figure, $\Delta\delta$ and $\Delta\ell$ are respectively normalized by the maximum CTOD, δs, and Δ_m corresponding to a stationary crack of the same depth subjected to the same stress. The arrowed

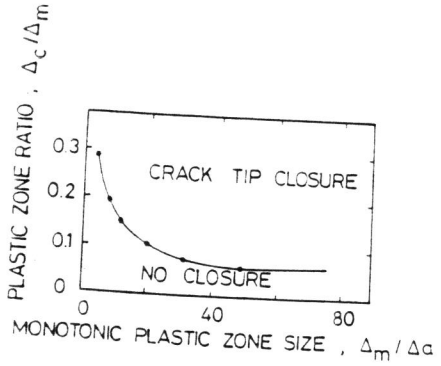

Fig. 9. Regimes of tip closure of a propagating fatigue crack.

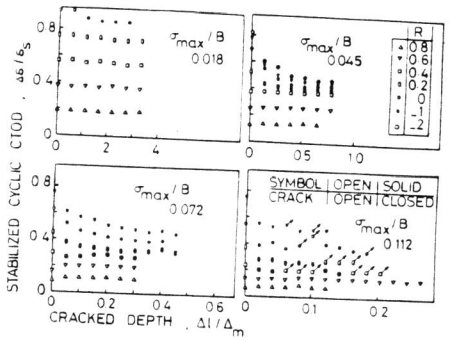

Fig. 10. Cyclic CTOD of a propagating fatigue crack against the additional cracked length.

symbols indicate the occurrence of discontinuous closure behind the crack tip. In this case, surface closure near the crack tip took place whilst the crack tip remained open. As reported by **Fleck (1986)**, this discontinuity in closure is due to the formation of a material wedge on the crack flanks located just behind the initial position of the crack tip, see Fig. 8.c. The data shown in Fig. 10 reveal several points of interest. For the same value of Δ_c/Δ_m the ratio of $\Delta\delta/\delta_s$ decreases as δ_s increases should the comparison be made at the same $\Delta l/\Delta_m$. In the cases where crack tip closure took place the ratio $\Delta\delta/\delta_s$ decreased to a stabilized value with the increase in cracking length. In spite of its stabilization, $\Delta\delta/\delta_s$ increased with the increase in cracking length in the cases resulting in no crack tip closure.

Data relevant to the stabilized opening stress for different maximum stresses and stress ratios, R, were obtained. For loading cycles having a constant R, the ratio of the stabilized opening stress and the applied maximum stress, σ_{op}/σ_{max}, decreased with the increase in σ_{max}. An increase in σ_{op}/σ_{max} was associated with an increase in R for a constant value of σ_{max}. Generally, this is in agreement with similar results in the literature (**McClung, 1991**; **Llorca and Galvez, 1989**).

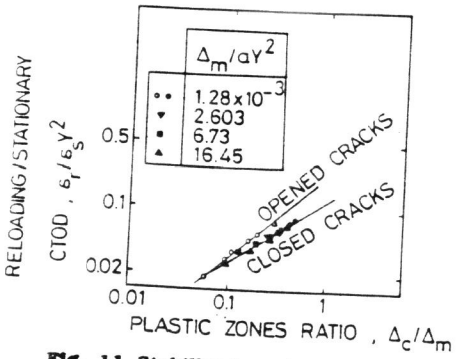

Fig. 11. Stabilized maximum CTOD of a propagating fatigue crack at the termination of the reloading phase.

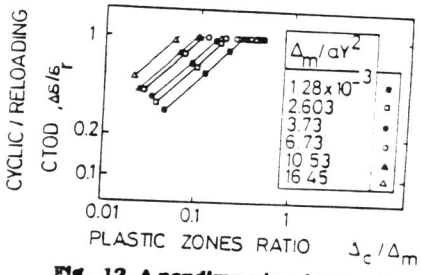

Fig. 12. A nondimensional presentation of the stabilized cyclic CTOD of a propagating fatigue crack

In consideration of stabilization the maximum CTOD at the termination of reloading, δ_r, was generally found less than δ_s as presented in Fig. 11 for cracks having either an opened or a closed tip. The effect of crack tip closure here is to reduce the ratio of δ_r/δ_s. Further, should crack tip close the cyclic CTOD, $\Delta\delta$, equals δ_r. This is illustrated in the type of correlating $\Delta\delta$ presented in Fig. 12 for the different cases analysed in the present work. For opened crack tips, i.e. $\Delta\delta < \delta_r$, the following equation could be obtained for $\Delta_m/\Delta a \leq 50$;

$$\Delta\delta/\delta_r = 24.58\,(\Delta_m/aY^2)^{0.39}\,(\Delta_c/\Delta_m)^{0.645} \qquad (2)$$

Otherwise, $$\Delta\delta/\delta_r = (16\,\Delta_c/\Delta_m)^{0.645} \qquad (3)$$

Following the mechanism of FCG, its correlation with CTD is advantageous. In Fig. 13 $\Delta\delta$ and δ_s/δ_r were utilized to conclude a meaningful function found suitable to present the FCG rates of geometrically different specimens made of three materials tested at different stress ranges and R-ratios (**Ohta et al, 1978**; **Chand and Garg, 1985**; **Kumar and Garg, 1989**). The ratio δ_s/δ_r represents the contribution of crack tip opening and blunting. As this ratio increases FCG rate is expected to increase.

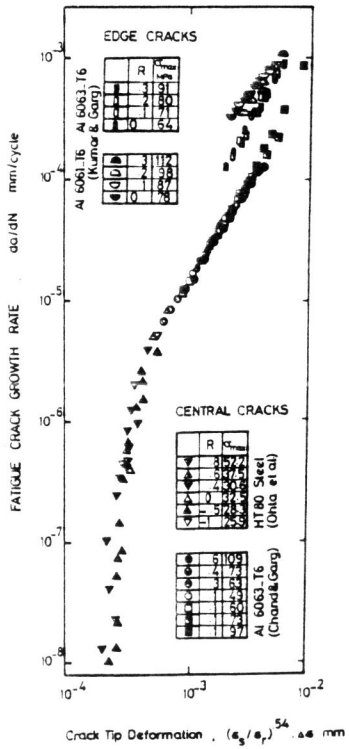

Fig. 13. Present correlation of FCG experimental data with CTD

CONCLUSIONS

An elastic-plastic finite element simulation of crack tip deformation in fatigue made it possible to conclude a meaningful factor capable of correlating fatigue crack growth of different materials tested at different stress ranges and ratios. This factor accommodates cyclic deformation at the propagating crack tip and the contribution of crack tip opening and blunting.

REFERENCES

Bowman, R., Antolovich, S. and Brown, R. (1988). Engng. Fract. Mech., 31. 703-712.
Fleck, N. (1986). Engng. Fract. Mech., 25, 441-449.
Llorca, J. and Galvez, V. (1989). ICF7, 2, 1229-1237.
McClung, R. (1991). Fatigue Fract. Engng. Mater. Struct., 14, 455-468.
Chand, S. and Garg, S. (1985). Engng. Fract. Mech., 21, 1-30.
Kumar, R. and Garg S. (1989). Engng. Fract. Mech., 32, 195-202.
Nakamura, H. Kobayashi, H., Yanase, S. and Nakazawa H. (1989). ICM4, 2, 817-823.
Newman, J. (1976). ASTM STP 590, 281-301.
Ohji K. Ogura K. and Ohkubo, Y. (1975). Engng. Fract. Mech., 7, 456-464.
Ohta, A., Kosuge, M. and Sasaki, E. (1978). Int. J. of Fracture, 14, 251-264.
Suzuki, N. Takeda, H., Ohta, A. and Ohuchida, H. (1991). Fatigue Fract. Engng. Mater. Struct., 14, 815-821.
Tanaka, K., Hoshide, T. and Sakai, N. (1984). Engng. Fract. Mech., 19, 805-825.
Tomkins, B. (1991). A lecture given in the course M2001 on Metal Fatigue. Department of Mechanical and Process Engineering, The University of Shiffield and SIRIUS.
Ziegler, H. (1959). Q. Appl. Math. 17, 55-65.